Desalination and Water Treatment
www.deswater.com
doi: 10.1080/19443994.2014.940386

56 (2015) 752–759
October

Taylor & Francis
Taylor & Francis Group

Effect of TiO_2 contents on the crystallization kinetics of PVDF in PVDF-diluent-TiO_2 blends

Yuxin Ma[a,*], Fengmei Shi[b], Jun Ma[b,]

[a]*College of Architecture and Civil Engineering, Heilongjiang University, Harbin 150080, China, Tel./Fax: +86 451 86604021; email: oucmyx@126.com*
[b]*State Key Laboratory of Urban Water Resource and Environment, School of Municipal and Environmental Engineering, Harbin Institute of Technology, Harbin 150090, China, Tel./Fax: +86 451 86283010; emails: ocean-water@126.com (F. Shi), majun@hit.edu.cn (J. Ma)*

Received 28 November 2013; Accepted 22 June 2014

ABSTRACT

Effect of TiO_2 contents on the non-isothermal crystallization kinetics of poly(vinylidence fluoride) (PVDF) in PVDF-diluent–TiO_2 blends was studied via differential scanning calorimetry method. Non-isothermal crystallization of PVDF was investigated by Jeziorny analysis and crystallizability analysis. Studies showed that the crystallization peak temperature of the blends increased from 363 to 375.6 K and the Avrami exponent decreased from 4 to 2.68, with the increase in TiO_2 content from 0 to 3.0 wt%. Higher TiO_2 content could hinder the growth of PVDF crystals in the blends. The blends with the TiO_2 content of 0.45% had the largest crystallization rate ($Z_c = 0.97$) and the maximum crystallizability ($G_R = 1.05$). Hopefully, the introduction of TiO_2 to the membrane mixture would be applied to control and adjust the structure of the membrane prepared.

Keywords: Crystallization kinetics; Nonisothermal crystallization; PVDF; TiO_2

1. Introduction

Crystallization plays an important role in the membrane formation process via Thermally Induced Phase Separation (TIPS) method, and has a great impact on the structure and performance of the membrane prepared. Many factors that influence the crystallization process such as quenching temperature [1], cooling rate and polymer-dilute composition [2] were studied in the polymer-dilute binary system. The increase in cooling rate resulted in the increase in crystallization rate [1,2]. Slower cooling rate favoured the growth and mature of the crystals, and lower quenching temperature, which was below the monotectic point, led to higher crystallization rate and crystallinity. β-phase poly(vinylidence fluoride) (PVDF) could be obtained by quenching PVDF–dimethyl phthalate (DMP) blends in liquid nitrogen and α-phase PVDF was formed by quenching PVDF–DMP blends to different temperatures above 40°C from melting at high temperature [1]. The viscosity of the system, the interaction between polymer and diluent, and the varying composition of polymer and dilute affected the crystallizing rate. Higher viscosity restrains the polymer molecule segments moving towards the crystal's surface [2].

PVDF is a semi-crystalline material suitable for the fabrication of ultrafiltration and microfiltration membranes. In order to meet the needs of special uses or

*Corresponding author.

to improve its innate hydrophilic properties, many inorganic or organic materials such as polymethyl methacrylate (PMMA) [3,4], polyvinyl alcohol [4], SiO_2 [5], $CaCO_3$ [6] and TiO_2 were introduced into the PVDF membranes [7–9]. Cui et al. [3] found that the addition of PMMA could increase the porosity and decrease the crystallinity of PVDF. The PMMA was an amorphous polymer that acted as a diluent because of its good compatibility with PVDF molecules [4]. PMMA could hinder the crystallization of PVDF during the crystallization process of PVDF. The addition of SiO_2 and $CaCO_3$ could influence the formation of PVDF crystals and affect the morphology and properties of membranes prepared via TIPS method [5,6]. In our previous studies [8,9], the introduction of TiO_2 could have an impact on the morphology, performance, thermal and mechanical properties of PVDF membranes, and the quenching temperature plays an important role in the formation of spherulitic crystal in the TIPS process. The nano-TiO_2 particles added to the PVDF–DMP mixtures affect the crystallization temperature, the melting temperature and the crystallinity of hybrid membranes prepared. Crystal nuclei are formed by homogeneous nucleation for PVDF membrane and by heterogeneous nucleation for PVDF/TiO_2 hybrid membranes. The addition of TiO_2 particles affect the number and the size of the spherulites in the membranes and could accelerate the crystallization rate and restrain the growth of (020) plane of PVDF. Spherulitic crystal formed in the membrane formation process would affect the structure and performance of the membrane prepared (summarized in Table 1). In fact, the PVDF crystals formed in the PVDF-diluent–TiO_2 blends were different from those of the PVDF-diluent binary blends. It was necessary to study the effect of TiO_2 particles in the crystallization process of the ternary blends, which could understand the nature of the PVDF/TiO_2 membrane formation.

From the above literatures, the introduction of inorganic additives could affect the morphology and properties of the membranes prepared. The effect of the addition of inorganic particles on the PVDF crystallization should be considered in the PVDF-dilute-inorganic particle ternary system.

In this study, PVDF–DMP–TiO_2 blends and PVDF/TiO_2 hybrid membranes were prepared with different nano-TiO_2 contents. Effects of nano-TiO_2 contents on the PVDF crystallization in the ternary mixtures were studied. The information gained from this study would be useful for the fundamental knowledge necessary to prepare PVDF porous hybrid membranes via TIPS method.

2. Experimental

2.1. Materials

PVDF (FR-904) ($M_n = 380, 000$) was purchased from Shanghai 3F new materials Co. Ltd Anatase titanium oxide (TiO_2) nanoparticle (average diameter 20 nm) was obtained from Meidilin Nanometer Material Co. Ltd. DMP was obtained from Shanghai Bio Life Science & Technology Co. Ltd. Ethanol used in the study was of AR grade.

2.2. Samples and membranes preparation

The preparation of PVDF–DMP–TiO_2 blends and hybrid membranes with different contents of nano-TiO_2 particles was presented in our previous study [8].

PVDF–DMP blends and neat PVDF membrane preparation: Measured amount of PVDF was added to 70% DMP in a beaker at the ambient temperature and mixed for seven minutes at 100 rpm of rotating speed. The beaker was mounted on an oil bath at 473 ± 5 K and the mixture was stirred for four hours at 50 rpm of rotating speed to form homogenous solution. The beaker was quenched in an ice-water bath for 10 min and a solid polymer–diluent sample were formed. The solid sample was chopped into small pieces and placed in a tailor-made steel plate, reheated to 473 K, and pressed into flat-sheet membranes. The membrane was quenched at 273 K ice–water bath. The diluent in the membrane was extracted by ethanol for 12 h and repeated for three times.

PVDF–DMP–TiO_2 blends and hybrid membrane preparation: Measured amount of TiO_2 nanoparticles

Table 1
Composition of the blends and the characteristics of the membrane prepared

Blends	Membranes prepared	PVDF (wt%)	TiO_2 (wt%)	DMP (wt%)	PWF ($L/m^2/h$)	Porosity (%)	Tensile strength (Mpa)	Elongation at break (%)
PDT-0	PT–0	30	0	70	63.44	58.83	1.4	16.5
PDT-0.45	PT–0.45	29.55	0.45	70	105.08	70.2	7.25	33.5
PDT −1.5	PT–1.5	28.5	1.5	70	86.369	52.88	5.47	12.4
PDT −3	PT–3	27	3	70	72.99	49.6	2.43	6.6

was pre–dispersed in DMP in a beaker and sonolyzed for 10 min. The measured amount of PVDF was then added to TiO_2–DMP mixture at ambient temperature and then mixed for seven minutes at 100 rpm of rotating speed. The other procedures were same to the PVDF–DMP blend and neat PVDF membrane samples preparation. The prepared blends and membrane samples were used for testing and subsequent characterization. The composition of the blends was presented in Table 1.

2.3. Samples and membranes characterization

A NETZSCH STA 449 C differential scanning calorimetry (DSC) analysis was used to study the melting and crystallization behaviour of the blend samples. The solid samples used in the study were cut from the central part of the blends, which were representive of PVDF–DMP or PVDF–DMP–TiO_2 mixtures. The temperature and energy scales were calibrated with the standard procedures. Blend samples were heated to 473 K first at a rate of 10 K/min in nitrogen atmosphere and held there for 10 min. Then, it was cooled to 298 K in nitrogen environment at the same rate. Crystallization parameters were obtained from cooling process.

The morphologies of spherical crystals were observed from the cross section of the membranes prepared because the growth of spherical crystals in the membrane surface was refrained by the moulds. The morphologies of spherical crystals were observed by a FEI Phenom Deskcope SEM. Membranes were fractured in liquid nitrogen and coated with a thin layer of gold by sputtering before observation.

A wide-angle X-ray diffraction (XRD) study of the membranes was conducted with a Dmax-rB X-ray diffractometer under a voltage of 40 kV and a current of 30 mA using Cu K_α radiation ($\lambda = 0.154$ nm). All samples were analysed in continuous scan mode with the 2 theta from 10° to 80°.

3. Result and discussion

3.1. Crystalline study

PVDF membranes fabricated by TIPS method in this study were isotropic. Crystalline studies could provide information about the crystallization process, crystal morphology, the melting or crystallization enthalpy, crystallinity, etc., which was important for PVDF membrane preparation.

In order to investigate the effects of TiO_2 contents on the crystallization process of PVDF, the blends with 0, 0.45, 1.5 and 3 .0 wt% TiO_2 contents were heated quickly to 493 K, and then cooled at the rate of 10 K/min to the ambient temperature. The DSC thermograms of PVDF–DMP–TiO_2 blends with different TiO_2 contents were shown in Fig. 1. The relative crystallization parameters obtained from Fig. 1 were shown in Table 2. T_{on} was the onset point of crystallization and T_c was the peak point of crystallization. The enthalpy of PVDF (ΔH) in the cooling process was calculated as

$$\Delta H = \Delta H_1 / \Phi \quad (1)$$

Where ΔH_1 was enthalpy obtained from DSC cooling diagram, J/g. Φ was the weight fraction of PVDF in the blends. It could be seen that the peak temperature of crystallization (T_c) of PVDF appeared at higher temperature with the increase in TiO_2 content from 0 to 3.0 wt% at the same condition. The overall crystallization kinetics of polymer was mainly affected by nucleation rate and crystal growth rate during polymer crystallization process. T_c was mainly determined by the crystal growth rate and could attest the nucleating impact of nucleating agents on polymer by shifting to high temperature [10]. In the ternary system, when TiO_2 was at high weight fraction, it was difficult for crystals to grow faster resulting from activated polymer molecules at higher temperature and the hindrance of TiO_2 particles. The heterogeneous nucleation could explain the increase in T_c of PVDF–DMP–TiO_2 blends. It was consistent with the results of the other studies [11,12]. ΔH had little change for the blends with the TiO_2 content increased from 0 to 1.5 wt% and

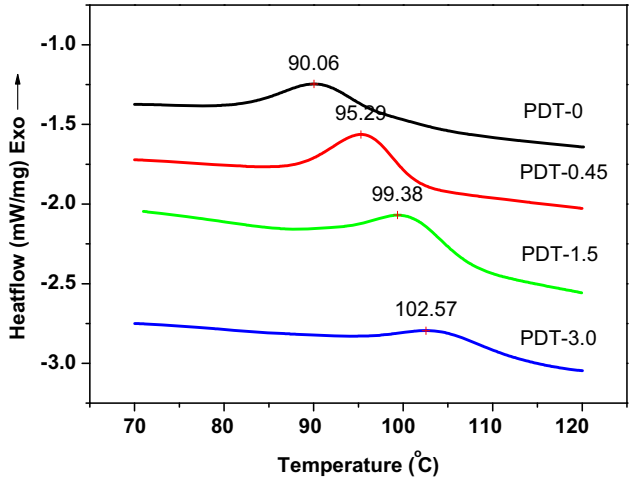

Fig. 1. DSC thermograms of PVDF–DMP–TiO_2 blends with different TiO_2 contents.

Table 2
Crystallization parameters of PVDF–DMP–TiO_2 blends with different TiO_2 contents at cooling rate of 10°C/min (Data obtained from Fig. 1)

TiO_2 content (wt %)	PDT-0	PDT-0.45	PDT-1.5	PDT-3.0
T_{on} (°C)	99.23	101.59	107.55	113.02
T_c (°C)	90.06	95.29	99.38	102.57
ΔH (J/g)	−47.68	−47.91	−47.81	−25.71

decreased for PDT-3.0. When the TiO_2 content was lower, nanoparticles were well distributed in the polymer matrix and the nuclei function was dominant. When the TiO_2 content was higher, TiO_2 agglomerations were found in the PVDF matrix and became a barrier to the growth of crystallization and hindered the arrangement of PVDF molecular chains. Higher content of TiO_2 particles hindered the growth of PVDF crystals.

PVDF crystal morphologies were obtained from the cross-sectional SEM images of the membranes. The PVDF crystal morphologies of the hybrid membranes with different TiO_2 contents were shown in Fig. 2. It could be seen that PVDF crystals in the membranes were spherical crystals which had sponge-like structure. The diameter of the crystals varied from 3–10 μm for PT-0 membrane to 3–5 μm for PT-0.45 membrane, then increased to 3–8 μm for PT-1.5 and 8–10 μm for PT-3. The pore sizes in the spherulites had no obvious change at the range of 0.2–0.8 μm. The PVDF crystal size of PT-0.45 membranes was more uniform than the others. The ultimate morphology of the crystals depended on the kinetics of nucleation and growth of the crystals. When there was no TiO_2 addition, the crystal nuclei were formed by homogeneous nucleation. The crystal nuclei that formed earlier grew to large crystals and the diameter of the crystals were not uniform. With the addition of TiO_2, the crystal nuclei were formed by heterogeneous nucleation. TiO_2 particles acted as crystal nuclei. With the increase in TiO_2 content, more nuclei were formed, and the diameter of spherulites decreased and became more uniform. When the TiO_2 content was high, TiO_2 particles aggregated in the polymer matrix even as a continuous phase. Growth of the crystallites was refrained by the aggregation of TiO_2 particles [8]. The addition of the nanoparticles affected the crystallization process and had an impact on the crystal size, so the membrane structure was influenced and the membrane prepared had distinct porosity (Table 1), which would affect their performance in the application process.

The XRD patterns of TiO_2, PVDF membrane and PVDF/TiO_2 hybrid membranes with different TiO_2 contents were presented in Fig. 3. For neat PVDF membrane, three discernible diffraction peaks appeared at 18.20°, 19.78° and 26.16° with reference to the diffractions in planes (020), (110) and (020) of α phase PVDF, respectively. The XRD curves of the PVDF/TiO_2 hybrid membranes had the well-defined peaks of α–phase PVDF [13–15]. The addition of

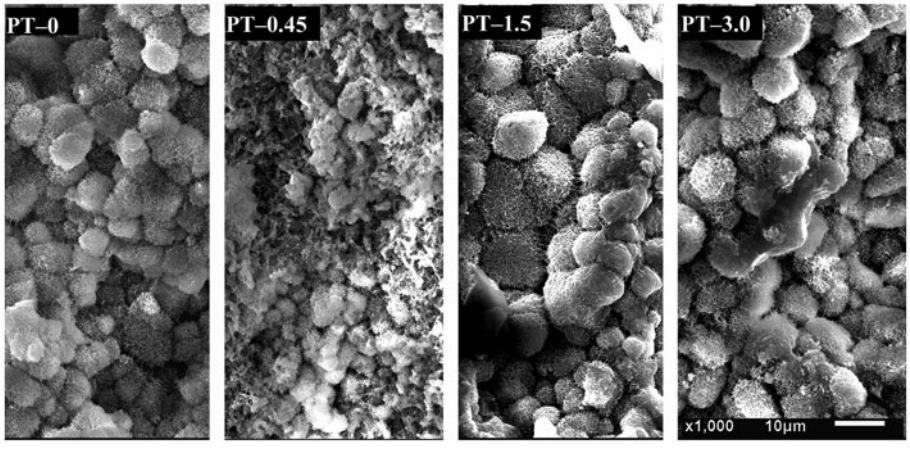

Fig. 2. PVDF crystal morphologies of hybrid membranes with different TiO_2 contents.

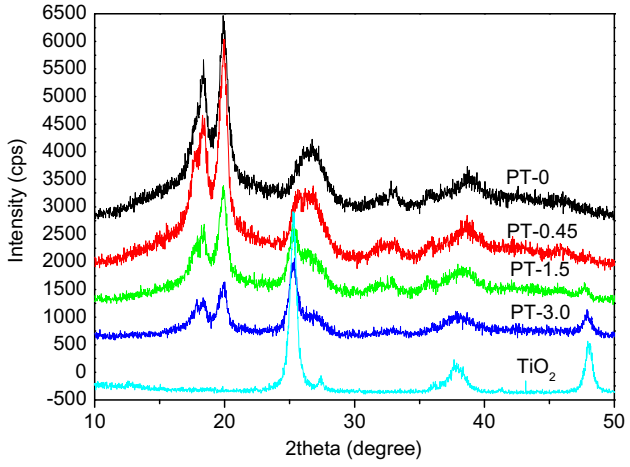

Fig. 3. XRD diffractograms of TiO_2, PVDF membrane and PVDF/TiO_2 hybrid membranes with different TiO_2 contents.

nanoparticles did not affect the crystalline phase of PVDF/TiO_2 hybrid membranes. The relative intensity ratios of (110) to (020) plane of α-phase for PVDF membranes with different TiO_2 contents were compared in Table 3. The relative intensity ratios of (110) to (020) plane of α-phase for PVDF and PVDF hybrid membranes were about 1.2 when the TiO_2 content was lower than 0.9 wt%, and increased with the further increase in TiO_2 content. It could be seen that the higher TiO_2 content restrained the growth of (020) plane of neat PVDF and hybrid membranes.

3.2. Non-isothermal crystallization analysis

Many models derived by extending the Avrami equation were proposed by Ozawa [16], Jeziorny [17], Ziabicki [18] and Liu [19] et al to interpret the non-isothermal crystallization kinetic of polymers. Among these models, Ozawa and Mo model could acquire crystallization kinetic parameters from several DSC curves [19]. It was difficult to obtain the crystallization rate parameters from Ozawa's equation because of the complexity of the crystallization rate function. It was very convenient to obtain crystallization kinetics parameters from one DSC curve of polymers using Jeziorny or Ziabicki model. In this paper, Jeziorny and Ziabicki methods were chosen to analyse the effect of TiO_2 contents on the crystallization kinetics such as crystallization rate and crystallizability of PVDF in PVDF-diluent–TiO_2 blends.

3.2.1. Jeziorny analysis

Jeziorny [17] used modified Avrami analysis to describe the non-isothermal crystallization kinetics of polymers. The relationship between relative crystallinity (X_T) and crystallization time (t) for non-isothermal crystallization is shown as Eqs. (2) or (3).

$$X_T = 1 - \exp(-Z_t t^n) \tag{2}$$

$$\log(-\ln(1 - X_T)) = n \log t + \log Z_t \tag{3}$$

Here n is the Avrami exponent, a mechanism constant depending on the nucleation type and growth process; Z_t is the Avrami rate constant, involving nucleation and growth parameters; and t is the crystallization time. Considering the process to be non-isothermal, Jeziorny [17] suggested that rate parameter Z_t should be corrected by cooling rate (R).

$$\log Z_c = \log Z_t / R \tag{4}$$

Here Z_c is the corrected crystallization constant.

When $X_T = 50\%$, Eq. (3) can be written as Eq. (5) and be used to calculate the crystallization half-time ($t_{1/2}$) values.

$$t_{1/2} = (\ln 2 / Z_t)^{1/n} \tag{5}$$

While the relative crystallinity (X_T) was calculated according to Eq. (6) [20].

$$X_T = \frac{\int_{T_0}^{T} (dH_c/dT)dT}{\int_{T_0}^{T_\infty} (dH_c/dT)dT} \times 100\% \tag{6}$$

Here T_0 and T_∞ were onset and end crystallization temperature, respectively. dH_c/dT was the heatflow rate.

Table 3
The relative intensity ratios of (110)–(020) plane of α phase for PVDF membrane and PVDF/TiO_2 hybrid membrane prepared with different TiO_2 contents

Hybrid membranes with different TiO_2 contents (wt%)	0	0.45	1.5	3.0
Intensity ratios of (110)–(020) plane	1.22	1.30	1.32	1.39

The values of n and Z_t or Z_c could be obtained from the slopes and intercepts of the straight-line of log $(-\ln (1 - X_T))$ vs. log t, respectively. The modified Avrami plots of log $(-\ln (1 - X_T))$ vs. log t the plots for PDT-0, PDT-0.45, PDT-1.5 and PDT-3.0 were shown in Fig. 4. The values of n, Z_t, Z_c and $t_{1/2}$ obtained from Fig. 4 were summarized in Table 4. The Z_c values of PDT-0.45, PDT-1.5 and PDT-3.0 blends were larger than that of PDT-3.0 blend. At the same cooling rate, the Avrami exponent n decreased with the increase in TiO_2 content. For PDT-0, n was about 4. It meant that the PVDF crystals grew in three-dimension (sphere geometry) corresponding to sporadic nucleation, while n was about 3 for PDT-0.45, PDT-1.5 and PDT-3.0 corresponding to three-dimensional growth (sphere geometry) for predetermined nucleation. With the TiO_2 content increased, the hindrance of TiO_2 agglomerations became more serious, and the growth of some crystal planes was refrained, which was also reflected in the XRD diffractograms (Fig. 3), so the n value decreased.

The values of Z_c increased from 0.78 to 0.97 with the TiO_2 content increased from 0 to 0.45 wt% in the blends and attained its maximum value, then decreased with the further increase in TiO_2 content. It took PDT-0.45 blends the shortest time to complete the crystallization process. The crystallization time became longer with the further increase in TiO_2 content. TiO_2 particles could accelerate the formation of PVDF crystals at lower content, but higher content of TiO_2 particles would form the TiO_2 agglomerations, which could restrict the movement of the polymeric segments to the growing crystal surface and reduce the growth rate of PVDF crystals. The crystallization process was decided by the acceleration function of TiO_2 particles as crystal nuclei and the hindrance function of TiO_2 agglomerations. The result was consistent with the crystal morphology study. More nuclei were formed in the quenching process for PDT-0.45 blends, and the blends formed more uniform crystal, so the crystal size was smaller and the crystallization time was shorter. For blends with higher TiO_2 content, the TiO_2 agglomerations affected the growth of PVDF crystal, the crystal size was irregular and the crystallization process was prolonged. The α-phase PVDF is stable at room temperature and could be transformed to β-phase PVDF via mechanical deformation, while the β-phase PVDF could be changed to α-phase PVDF under thermal treatment [21]. The PVDF molecules were not stretched or oriented during the TIPS process, so the PVDF crystalline phase was not changed.

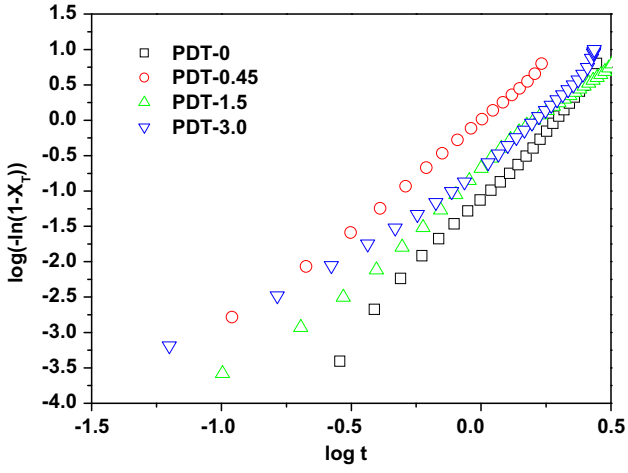

Fig. 4. The log $(-\ln[1 - X_T])$ vs. log t plots for PVDF–DMP–TiO_2 blends with different TiO_2 contents at 10°C/min cooling rate.

Table 4
The crystallization kinetics parameters of PVDF–DMP–TiO_2 blends with different TiO_2 contents at 10°C/min cooling rate (obtained from Fig. 4)

PVDF–DMP–TiO_2 blends	n	Z_t	Z_c	$t_{1/2}$ (min)
PDT-0	3.97	0.08	0.78	1.72
PDT-0.45	3.00	0.71	0.97	0.99
PDT −1.5	2.73	0.57	0.94	1.07
PDT −3.0	2.68	0.33	0.89	1.32

3.2.2. Kinetic crystallizability analysis

For a given cooling condition, Ziabicki[18] proposed a parameter kinetic crystallinity G to describe the crystallizability over the entire crystallization process. On the basis of Ziabicki model, Jeziorny [17] suggested that the crystallization rate function $K(T)$ could be described by a Gaussian function of the following form:

$$K(T) = K_{\max} \exp\left[\frac{-4 \ln 2 (T - T_{\max})^2}{D^2}\right] \quad (7)$$

where $T_{\max}$ was the temperature at which the crystallization rate is maximum, $K_{\max}$ was the crystallization rate at $T_{\max}$ and D was the width at half-height of the crystallization rate–temperature function. With the use of the isothematic kinetic approximation, integration of Eq. (7) over the whole crystallizable range of temperatures ($T_g < T < T_m^0$), for a given cooling condition, led to an important characteristic value for the crystallization

Table 5
Nonisothermal crystallization parameters for PVDF–DMP–TiO_2 blends with different TiO_2 contents at 10℃/min cooling rate based on Ziabicki's crystallizability analysis

PVDF–DMP–TiO_2 blends	T_{max} (℃)	D_R (℃)	X_{max} (min^{-1})	G	G_R
PDT-0	90.8	9.17	0.897	8.752	0.875
PDT-0.45	95.3	7.92	1.241	10.458	1.046
PDT-1.5	99.4	11.02	0.833	9.767	0.977
PDT −3.0	104.0	10.11	0.882	9.487	0.949

ability (G) of a semi-crystalline polymer, which was defined as.

$$G = \int_{T_g}^{T_m^0} K(T)dT = \left(\frac{\pi}{\ln 2}\right)^{\frac{1}{2}} \times K_{max} \times \frac{D}{2} \approx 1.064\, K_{max} D \tag{8}$$

According to the approximate theory [17], the kinetic crystallizability (G) characterized the degree of crystallinity obtained when the polymer was cooled at unit cooling rate from the melting temperature to the glass transition temperature [17]. In the case of non-isothermal crystallization studies using DSC where cooling rate was variable, Eq. (8) could be applied when the crystallization rate function $K(T)$ was replaced with a derivative function of the relative crystallinity $X(T)$ for a particular cooling rate R. The kinetic crystallizability at unit cooling rate G could be obtained by normalizing G_R with R ($G_R = G/R$) [22].Therefore, Eq. (8) was replaced by.

$$G_R = \int_{T_g}^{T_m^0} X(T)dT \approx 1.064 X_{max} D_R \tag{9}$$

where X_{max} and D_R were the maximum crystallization rate and the width at half-height of the derivative relative crystallinity as a function of temperature (T).

Table 5 summarized the values of T_{max}, X_{max} and D_R for PVDF–DMP–TiO_2 blends with different TiO_2 contents at 10 K/min cooling rate (obtained from Fig. 4). The values of X_{max} and D_R were used to calculate the Ziabicki's kinetic crystallizability G_R. The values of G_R were also summarized in Table 5. The practical meaning of G is the ability of a semi-crystalline polymer to crystallize when it is cooled from the melt to the glassy state at a unit cooling rate. hence the higher the G value is, the more readily the polymer can crystallize. According to Table 5, the G_R value for PVDF–DMP blends were found to be 0.875, while the G_R values were 1.046, 0.977, 0.949 for PDT-0.45, PDT-1.5, PDT-3.0, respectively, which were all greater than that of PVDF–DMP blends, suggesting that the PVDF–DMP–TiO_2 blends crystallized more easily than the PVDF–DMP blends. The crystallization process was composed of nuclei formation and crystal growth. A small amount of TiO_2 addition meant that a tremendous number of particles were introduced. This introduced significant amount of surface area and nucleated the PVDF around each particle. Therefore, this would accelerate the nuclei formation. The addition of TiO_2 beyond the 0.45 wt% formed more agglomerations. Therefore, the PVDF crystallization rate would decline. Higher TiO_2 content would form TiO_2 agglomerations, which could refrain the growth of crystal and lower the ability to crystallize. The results were consistent with the Jeziorny analysis.

4. Conclusions

The effect of TiO_2 contents on the non-isothermal crystallization kinetics of PVDF in PVDF-diluent–TiO_2 blends weas studied by Jeziorny analysis and Ziabicki's crystallizability analysis. The results were summarized as follows:

(1) The crystallization peak temperature increased with the increase in TiO_2 contents due to the heterogeneous nucleating functions of TiO_2.
(2) The TiO_2 addition did not affect the crystal phase of PVDF, but higher TiO_2 content could hinder the growth of PVDF crystals in the blends by restraining the growth of (020) plane.
(3) The Avrami exponent decreased with the increase in TiO_2 contents. The Avrami exponent showed that the PVDF crystals grew in three-dimensions. The crystal nuclei were formed by sporadic nucleation and predetermined nucleation for PVDF–DMP blends and PVDF–DMP–TiO_2 blends, respectively. Jeziorny analysis attested the heterogeneous nucleating functions of TiO_2.

(4) For PVDF–DMP–TiO_2 blends, the crystal formation was affected by the nucleation function of TiO_2 particles and the crystal growth process was also affected by the spacial hindrance function of TiO_2 agglomerations. The blends with the TiO_2 content of 0.45% had the largest crystallization rate ($Z_c = 0.97$) and the maximum crystallizability ($G_R = 1.05$).

Acknowledgements

This work was supported by the Scentific Research Funds of Heilongjiang Provincial Education Department [Grant number 12531503].

References

[1] M. Gu, J. Zhang, X. Wang, W. Ma, Crystallization behavior of PVDF in PVDF–DMP system via thermally induced phase separation, J. Appl. Polym. Sci. 102 (2006) 3714–3719.
[2] G. Ji, B. Zhu, C. Zhang, Y. Xu, Nonisothermal crystallization kinetics of poly(vinylidene fluoride) in a poly (vinylidene fluoride)/dibutyl phthalate/di(2-ethylhexyl)phthalate system via thermally induced phase separation, J. Appl. Polym. Sci. 107 (2008) 2109–2117.
[3] Z. Cui, Y. Xu, L. Zhu, X. Wei, C. Zhang, B. Zhu, Preparation of PVDF/PMMA blend microporous membranes for lithium ion batteries via thermally induced phase separation process, Mater. Lett. 62 (2008) 3809–3811.
[4] A. Linares, J.L. Acosta, Pyro-piezoelectrics polymers materials—I. Effect of addition of PVA and/or PMMA on overall crystallization kinetics of PVDF from isothermal and non-isothermal data, Eur. Polym. J. 31 (1995) 615–619.
[5] A. Cui, Z. Liu, C. Xiao, Y. Zhang, Effect of micro-sized SiO_2-particle on the performance of PVDF blend membranes via TIPS, J. Membr. Sci. 360 (2010) 259–264.
[6] X. Li, X. Lu, Morphology of polyvinylidene fluoride and its blend in thermally induced phase separation process, J. Appl. Polym. Sci. 101 (2006) 2944–2952.
[7] L. Shao, Z. Wang, Y. Zhang, Z. Jiang, Y. Liu, A facile strategy to enhance PVDF ultrafiltration membrane performance via self-polymerized polydopamine followed by hydrolysis of ammonium fluotitanate, J. Membr. Sci. 461 (2014) 10–21.
[8] F. Shi, Y. Ma, J. Ma, P. Wang, W. Sun, Preparation and characterization of PVDF/TiO_2 hybrid membranes with different dosage of nano-TiO_2, J. Membr. Sci. 389 (2012) 522–531.
[9] F. Shi, J. Ma, P. Wang, Y. Ma, Effect of quenching temperatures on the morphological and crystalline properties of PVDF and PVDF–TiO_2 hybrid membranes, J. Taiwan. Inst. Chem. Eng. 43 (2012) 980–988.
[10] S. Schneider, X. Drujon, J.C. Wittmann, B. Lotz, Impact of nucleating agents of PVDF on the crystallization of PVDF/PMMA blends, Polymer, 42 (2001) 8799–8806.
[11] K. Ke, Y. Wang, W. Yang, B. Xie, M. Yang, Crystallization and reinforcement of poly (vinylidene fluoride) nanocomposites: Role of high molecular weight resin and carbon nanotubes, Polym. Test. 31 (2012) 117–126.
[12] K. Asai, M. Okamoto, K. Tashiro, Crystallization behavior of nano-composite based on poly(vinylidene fluoride) and organically modified layered titanate, Polymer 49 (2008) 4298–4306.
[13] J. Kim, W. Cho, C. Ha, Morphology, crystalline structure, and properties of poly(vinylidene fluoride)/silica hybrid composites, J. Polym. Sci. B: Polym. Phys. 40 (2002) 19–30.
[14] J.R. Gregorio, M. Cestari, Effect of crystallization temperature on the crystalline phase content and morphology of poly(vinylidene fluoride), J. Polym. Sci. B: Polym. Phys. 32 (1994) 859–870.
[15] K. Pramoda, A. Mohamed, I. Phang, T. Liu, Crystal transformation and thermomechanical properties of poly(vinylidene fluoride)/clay nanocomposites, Polym. Int. 54 (2005) 226–232.
[16] T. Ozawa, Kinetics of non-isothermal crystallization, Polymer 12 (1971) 150–158.
[17] A. Jeziorny, Parameters characterizing the kinetics of the non-isothermal crystallization of poly(ethylene terephthalate) determined by d.s.c, Polymer 19 (1978) 1142–1144.
[18] A. Ziabicki, Kinetics of polymer crystallization and molecular orientation in the course of fiber spinning, Appl. Polym. Symp. 6 (1967) 1–18.
[19] T. Liu, Z. Mo, S. Wang, H. Zhang, Nonisothermal melt and cold crystallization kinetics of poly(aryl ether ether ketone ketone), Polym. Eng. Sci. 37 (1997) 568–575.
[20] F. Chivrac, E. Pollet, L. Avérous, Nonisothermal crystallization behavior of poly(butylene adipate-co-terephthalate)/clay nano-biocomposites, J. Polym. Sci. B: Polym. Phys. 45 (2007) 1503–1510.
[21] A.J. Lovinger, Crystallization of the β phase of poly (vinylidene fluoride) from the melt, Polymer 22 (1981) 412–413.
[22] P. Charoenphol, P. Supaphol, Nonisothermal melt-crystallization kinetics of syndiotactic polypropylene compounded with various nucleating agents, J. Appl. Polym. Sci. 95 (2005) 245–253.